

# Mechanism of $\text{La}_2\text{O}_3$ as combustion improver in blast furnace coal injection

Yanqin Sun<sup>1,2</sup> · Bing Hu<sup>1,2</sup> · Qing Lü<sup>1,2</sup> · Shuhui Zhang<sup>1,2</sup>

Received: 10 September 2015/Revised: 26 October 2015/Accepted: 29 November 2015/Published online: 9 March 2016  
© The Author(s) 2016. This article is published with open access at Springerlink.com

**Abstract**  $\text{La}_2\text{O}_3$  is a combustion improver suitable for burning pulverized coal in blast furnace.  $\text{La}_2\text{O}_3$  forms the active species  $\text{La}^{3+}(\text{CO}^-)_3$  that weakens the bridge adhesion of carbon structural units and alters the lattice structures, thus reducing the activation energy of the pulverized coal and accelerating the burning process. Research shows that  $\text{La}_2\text{O}_3$  can form the active species  $\text{La}^{3+}(\text{CO}^-)_3$ , which weakens the bridge adhesion of carbon structural units and alters the lattice structures of the fixed carbon, hence decreasing the activation energy of the pulverized coal and accelerating the burning process.

**Keywords** Combustion improver ·  $\text{La}_2\text{O}_3$  · Microcrystalline parameter · Average particle diameter · Morphological appearance

## 1 Introduction

The catalytic effect of  $\text{La}_2\text{O}_3$  has been studied (Wang and Shen 2001; Shi and Wang 2013). Increasing the injection of coal powder into blast furnace will reduce the combustion rate of pulverized coal in the raceway, increase unburned coal, and decrease the layer permeability of the blast furnace, all of which seriously impede the efficient operation of the blast furnace. The addition of combustion improver into pulverized coal can improve the combustion rate and reduce unburned coal in the furnace interior, which facilitates slag–iron separation and improves the efficiency of the blast furnace.  $\text{La}_2\text{O}_3$  is a pulverized coal combustion improver suitable for blast furnace. When a proper amount of  $\text{La}_2\text{O}_3$  is blended with pulverized coal, the combustion is accelerated, the coal injection amount

and the coal-to-coke replacement ratio are both enhanced, and the production cost of steel is reduced. The mechanism of  $\text{La}_2\text{O}_3$  as a combustion improver in blast furnace coal injection has been inadequately studied thus far (Indronil and Muthukuma 2000; Assis et al. 2004; Mathieson et al. 2005; Liang et al. 2007; Gong et al. 2009; He et al. 2012).

## 2 Experimental

### 2.1 Material

The coal injected into the blast furnace was a pulverized mixture of bituminous coal and anthracite coal, the compositions of which are shown in Table 1. The pulverized coal mixture contained 30 % No. 1 anthracite coal, 30 % No. 2 anthracite coal, and 40 % bituminous coal. The particle size of the pulverized coal mixture was less than 0.074 mm. The blended formulation contained 99 g pulverized coal mixture and 1 g reagent grade  $\text{La}_2\text{O}_3$ , which were mixed in a ball mill and dried in an oven at 105 °C for 1 h.

The influence of  $\text{La}_2\text{O}_3$  on the combustion of the pulverized coal in the pulverized coal mixture was evaluated

✉ Qing Lü  
lq@heuu.edu.cn

<sup>1</sup> College of Metallurgy and Energy, Hebei United University, Tangshan 063009, China

<sup>2</sup> Hebei Key Laboratory for Advanced Metallurgy Technology, Tangshan 063009, China

**Table 1** Proximate and ultimate analyses of coal sample

| Coal                  | Proximate analysis (%) |       |          |          | Ultimate analysis (%) |      |      |       |      |
|-----------------------|------------------------|-------|----------|----------|-----------------------|------|------|-------|------|
|                       | Fixed carbon           | Ash   | Volatile | Moisture | C                     | H    | N    | O     | S    |
| Bituminous coal       | 55.07                  | 10.92 | 28.48    | 5.53     | 60.46                 | 4.72 | 1.12 | 14.96 | 0.40 |
| No. 1 anthracite coal | 77.54                  | 11.73 | 9.91     | 0.82     | 78.91                 | 3.66 | 0.80 | 3.65  | 0.43 |
| No. 2 anthracite coal | 80.22                  | 10.62 | 8.12     | 1.04     | 79.46                 | 3.27 | 0.73 | 4.39  | 0.49 |

Both analyses use air dried samples

by thermogravimetry and differential thermal analysis. The unburned coal was examined using X-ray diffraction (XRD) and scanning electron microscope (SEM) to determine the changes in the functional groups and microscopic structure of the unburned coal when using  $\text{La}_2\text{O}_3$  as the improver.

## 2.2 Equipment

The experimental device consisted of two vertical electric furnaces as shown in Fig. 1. In the combustion experiments, 40 g pulverized coal was put in the bottle and the hot gas flow and blowing gas flow were set at 0.5–0.8  $\text{m}^3/\text{h}$  and 0.8–1.0  $\text{m}^3/\text{h}$ , respectively. The injection time was set to approximately 15 min to ensure the even combustion of the pulverized coal. Unburned coal powders were collected after the injection was finished. The injection system was purged with air before running the next experiment to remove the pulverized coal that remained in the pipe of the blast furnace. All tests were done in replicates to reduce error. This experimental device allowed continuous injection, which could simulate the coal injection process of blast furnace and improve the accuracy of the test results.

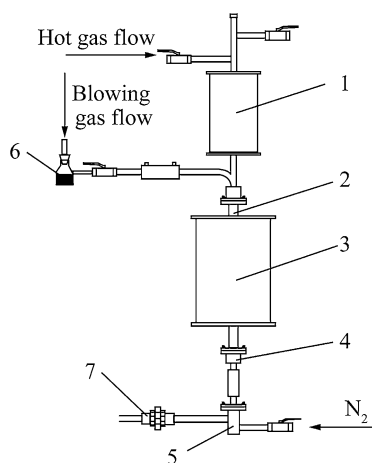


**Fig. 1** Combustion experiment set-up 1 air heater; 2 alundum tube; 3 combustion furnace; 4 coolant system; 5 ash tank; 6 pulverized coal bottle; 7 dust remover

## 3 Results and analysis

### 3.1 Influence of $\text{La}_2\text{O}_3$ on the combustion of fixed carbon

The coal combustion in the presence of  $\text{La}_2\text{O}_3$  was evaluated by thermogravimetry and differential thermal analysis using an STA409C analyzer (NETZSCH, German). The DTA and TG curves are shown in Figs. 2 and 3. The characteristic temperature points are listed in Table 2.

Table 2 shows that the inflection point temperature of the  $\text{La}_2\text{O}_3$  blended pulverized coal, which represents the initial release of volatile compounds, decreased by 18.3  $^\circ\text{C}$  compared with that of the raw coal. Besides, the first peak point (the combustion of volatile compounds) and the second peak point (the delayed release of volatile compounds) of the  $\text{La}_2\text{O}_3$  blended pulverized coal also decreased by 22.7 and 2.3  $^\circ\text{C}$  respectively. This is because the combustion of carbon is a gas–solid two phase reaction. Electromotive force exists on the contact surface between the reactants of the two phases. Because  $\text{La}^{3+}$  has empty d and f orbits to accept lone pair electrons, unsaturated oxygen-containing hydrocarbon functional groups could grow together and form  $\text{La}^{3+}(\text{CO}^-)_3$  species on the fixed carbon (complex salt). This can reduce the potential energy barrier between reactants of the two phases and decrease

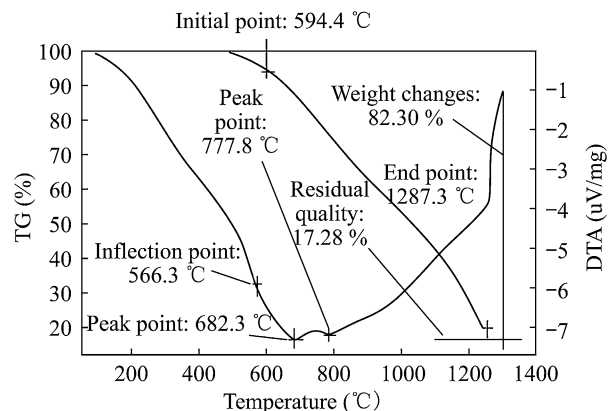


**Fig. 2** DTA and TG curves of raw coal's fixed carbon

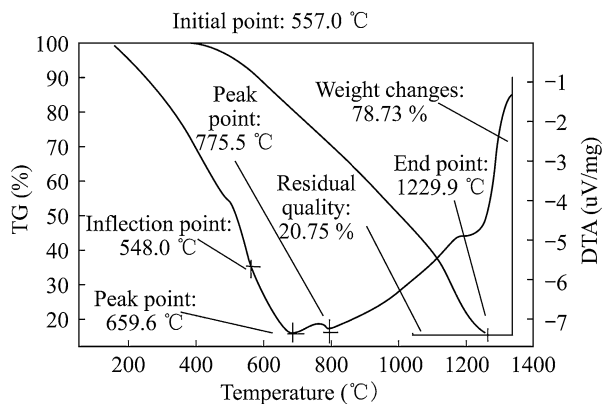


**Fig. 3** DTA and TG curves of coal blended with La<sub>2</sub>O<sub>3</sub>

the activation energy of the reactants, which thus reduces the temperature of the initial release of volatile compounds (Thoms et al. 1996; Morimasa et al. 2001).

During the thermal decomposition, La<sup>3+</sup>(CO<sub>3</sub>)<sub>3</sub> weakened the bridge adhesion of carbon structural units and changed the lattice structures. As a result, the embedded volatile compounds were more easily released. Consequently, the La<sub>2</sub>O<sub>3</sub> improver could effectively shorten the combustion reaction of the fixed carbon and accelerate the burning of the pulverized coal.

Table 2 shows that compared with the raw coal, the La<sub>2</sub>O<sub>3</sub> blended pulverized coal decreased by 37.4 °C in the ignition temperature and by 57.4 °C in the burning out point temperature. These results are related with the combustion characteristics of the blast furnace raceway, where carbon is in excess and oxygen falls short. Both the burning time (10 ms or less) and the burning space are strictly limited. The addition of La<sub>2</sub>O<sub>3</sub> decreases the ignition point temperature and the burning out point temperature of fixed carbon, thus facilitating the combustion of the pulverized coal. The TG experiment showed that the combustion window of the fixed carbon is 692.9 °C in the raw coal but reduced to 672.9 °C after the addition of La<sub>2</sub>O<sub>3</sub> to the pulverized coal, which proves that La<sub>2</sub>O<sub>3</sub> improved the combustion efficiency of fixed carbon.

The weight loss rate and residual weight are 82.3 and 17.3 % for raw coal and 78.7 and 20.8 % for La<sub>2</sub>O<sub>3</sub> blended pulverized coal, respectively. Because the pulverized coal adsorbed atmospheric species in the beginning

of the combustion reaction, which caused weight gain, the sum of weight loss rate and residual weight would be less than 100 %. Compared with raw coal, the weight loss rate of La<sub>2</sub>O<sub>3</sub> blended pulverized coal is slightly lower and the residual weight is higher, mainly because the majority of La<sub>2</sub>O<sub>3</sub> residue entered into the ash. Deducting La<sub>2</sub>O<sub>3</sub> from the ash shows that the fixed carbon weight loss rate was almost unchanged. La<sub>2</sub>O<sub>3</sub> only lowered the fixed carbon ignition temperature and improved the fixed carbon burning speed. Therefore, it can be concluded that for coal injection into blast furnace, using La<sub>2</sub>O<sub>3</sub> as an improver can shorten the burning time of pulverized coal, reduce unburned coal, and also further improve coal-to-coke replacement.

### 3.2 Influence of the combustion improver La<sub>2</sub>O<sub>3</sub> on unburned coal

#### 3.2.1 XRD comparisons

The X-ray diffraction can reveal changes in the microstructure of unburned coal powder. The shape and size of the cells determine the diffractive direction (Lu 2001; Gong and Guo 2009). The diffraction intensity is determined by the atom arrangement in the cell. The peak (002) and (100) represent the aromatic stack height (microcrystalline parameter  $L_c$ ) and the layer diameter (microcrystalline parameters  $L_a$ ), which can be calculated from the Scherrer equation (Burton et al. 2009).

$$L_c = \frac{K_1 \lambda}{\beta(002) \cos \theta(002)} \quad (1)$$

$$L_c = \frac{K_2 \lambda}{\beta(100) \cos \theta(100)} \quad (2)$$

where  $\lambda = 0.154178$  nm is the X-ray wavelength,  $\theta$  is the Bragg angle;  $\beta$  is the FWHM of the peak (002) and (100), and  $K_1 = 0.94$  and  $K_2 = 1.84$  are the Scherrer constant.

After combustion, the unburned raw coal and the unburned La<sub>2</sub>O<sub>3</sub> blended pulverized coal were collecting from the furnace and analyzed by XRD. The XRD spectra are shown in Figs. 4 and 5. The microcrystalline parameters of the unburned coals are listed in Table 3.

**Table 2** Characteristic temperature points in the DTA curves

| Sample   | Inflection point (°C) | First peak point (°C) | Second peak point (°C) | Ignition temperature (°C) | Burning out point temperature (°C) | Weight loss rate (%) | Residual weight (%) |
|--|-----------------------|-----------------------|------------------------|---------------------------|------------------------------------|----------------------|---------------------|
| Raw coal   | 566.3                 | 682.3                 | 777.8                  | 594.4                     | 1287.3                             | 82.3                 | 17.3                |
| Coal blended with La <sub>2</sub> O <sub>3</sub> | 548.0                 | 659.6                 | 775.5                  | 557.0                     | 1229.9                             | 78.7                 | 20.8                |

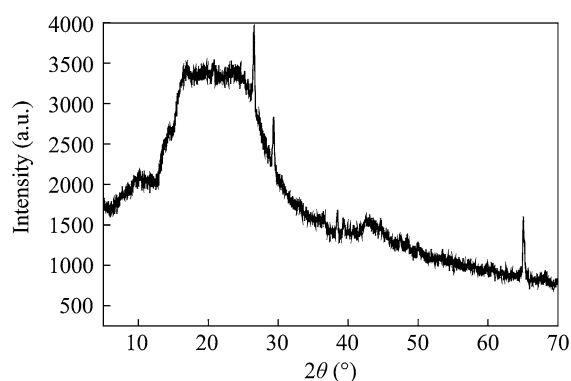


**Fig. 4** XRD spectrum of unburned raw coal

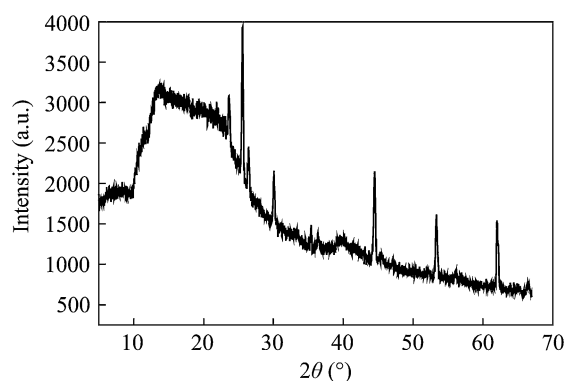


**Fig. 5** XRD spectrum of unburned  $\text{La}_2\text{O}_3$  blended coal

**Table 3** Microcrystalline parameters of unburned coal

| Sample  | $d_{(002)}$ (nm) | $L_c$ (nm) | $L_a$ (nm) |
|---|------------------|------------|------------|
| Unburned raw coal                             | 0.3776           | 1.2337     | 2.5165     |
| Unburned $\text{La}_2\text{O}_3$ blended coal | 0.3481           | 1.2384     | 2.5545     |

Figures 4 and 5 show that the diffraction intensities of the peak (002) and (100) in the XRD spectra are enhanced after the addition of the combustion improver  $\text{La}_2\text{O}_3$ , *i.e.*, the peak height is increased and the peak shape is sharpened. The microcrystalline parameter  $L_c$  of the unburned  $\text{La}_2\text{O}_3$  blended pulverized coal is 1.2384 nm, which is 0.0047 nm larger than that of unburned raw coal. The addition of  $\text{La}_2\text{O}_3$  also enlarged the aromatic layer diameter by 0.0380 nm, from 2.5165 to 2.5545 nm. This is because  $\text{La}_2\text{O}_3$  promotes the growth of the active particle  $\text{La}^{3+}(\text{CO}^-)_3$ . The aromatic nucleus carbon and the aliphatic carbon chain of the pulverized coal can easily combine with  $\text{La}^{3+}(\text{CO}^-)_3$ .  $\text{La}^{3+}(\text{CO}^-)_3$  then delivers oxygen to the carbon ring and the carbon chain by the electronic effect of  $\text{La}^{3+}$ . The large molecules and the branched chains of the aromatic rings are ruptured to generate CO and  $\text{CO}_2$ , thus decreasing the proportion of

non-aromatic structures in the unburned coal. Meanwhile,  $\text{La}^{3+}(\text{CO}^-)_3$  could also promote the dehydrogenation polycondensation reaction. Only the aromatic nucleus that has high degree of polymerization was dehydrogenated and turned into unburned coal, thus increasing the microcrystalline parameters of unburned coal.

In addition, pulverized coals were heated rapidly at high temperatures and generated plenty of  $\text{sp}^2$  hybridized carbon atoms (carbon free radicals) and  $\text{C}^*$  fragments. These fragments could not react timely in the combustion furnace and became coke, which also increased the microcrystalline parameters of the unburned coal (Takanohashi et al. 1999; Akiyama 2000; Michael 2002).

### 3.2.2 SEM comparisons

Using scanning electron microscopes (SEM) allows directly observing the void structure and the three-dimensional molecular structure of coal. The unburned coals were examined using scanning electron microscopes and the morphological changes after the addition of  $\text{La}_2\text{O}_3$  to the pulverized coal were analyzed. In order to prepare the sample for SEM analysis, the unburned coal was first dispersed in alcohol to remove surface dirt and impurities, then placed on conducting resin and dried at room temperature. Afterwards, the 10-nm thick gold conductive layer was sprayed using an ion sputtering coating instrument. The samples were analyzed sequentially to determine the average particle diameters. The scanning electron micrographs are shown in Figs. 6 and 7.

Figures 6 and 7 show that the average particle diameter of unburned raw coal is 6.08  $\mu\text{m}$ , whereas the average particle diameter of unburned  $\text{La}_2\text{O}_3$  blended pulverized coal is decreased by 2.61 to 3.47  $\mu\text{m}$ . Moreover, the morphological appearance of unburned  $\text{La}_2\text{O}_3$  blended pulverized coal became irregular.  $\text{La}_2\text{O}_3$  ruptured large molecules and the branched chain of aromatic rings to form small molecules and radical fragments, which could escape

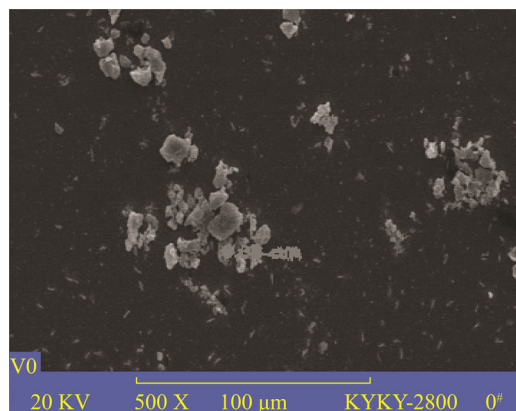


**Fig. 6** SEM of unburned raw coal

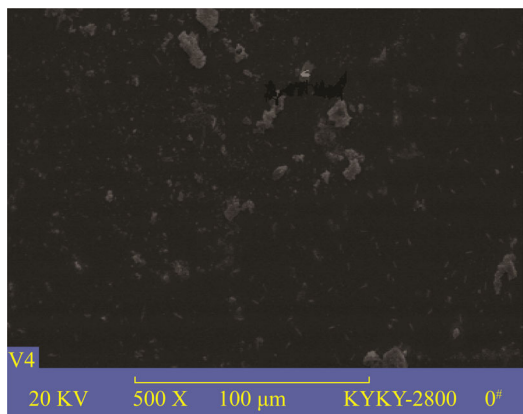


**Fig. 7** SEM of unburned La<sub>2</sub>O<sub>3</sub> blended pulverized coal

from coal particles along the non-covalent bond parts in the aromatic polymer accumulation. These parts formed channels and fissures that increased the surface area of coke particles after burning. Hence, coke particles could more easily combine with oxygen, and the combustion rate of the pulverized coal would be increased. Besides, the porosity of coke particles grew continuously, which resulted in the formation of smaller fragments. Therefore, the addition of the La<sub>2</sub>O<sub>3</sub> combustion improver reduced the average particle diameter of unburned coal.

The combustion process of pulverized coal has three stages: (1) evaporation of volatile materials, (2) combustion of volatile materials and (3) burning of fixed carbon. In the first stage, volatile materials adsorbed to the coal particles were heated and evaporated mainly by travelling through the existing holes. At this stage there is no plastic deformation and the surface of the coal particles has no obvious change. Therefore, the La<sub>2</sub>O<sub>3</sub> combustion improver has little influence on the evaporation of volatile materials. In the second stage and the third stage, the combustion of volatile materials produced significant amount of heat, which was transmitted to fixed carbon particles and lead to plastic deformation. The volatile materials inside the coal particles were heated, evaporated, expanded and burned, during which the intense combustion and heat transfer generated new holes on the surface of coal particles and increased their fractal dimension (Ishii 2000; Ichida et al. 2000; Mathieson et al. 2005). Consequently, the average particle diameter of unburned coal was reduced and the morphological appearance became irregular. It can be concluded that La<sub>2</sub>O<sub>3</sub> plays an important role in promoting the combustion of both volatile material and fixed carbon.

#### 4 Conclusions

- (1) The combustion improver La<sub>2</sub>O<sub>3</sub> can form the active species La<sup>3+</sup>(CO<sup>-</sup>)<sub>3</sub>, which weakens the bridge

adhesion of carbon structural units and alters the lattice structures of the fixed carbon, hence decreasing the activation energy of the pulverized coal and accelerating the burning process.

- (2) The XRD spectra show that the addition of the combustion improver La<sub>2</sub>O<sub>3</sub> increased the stack height and the aromatic slice diameter of the unburned coal by 0.0047 and 0.0380 nm, respectively.
- (3) The SEM images show that after the addition of the combustion improver La<sub>2</sub>O<sub>3</sub>, the average particle diameter of the unburned coal decreased by 2.61 μm and the morphological appearance became irregular.

**Acknowledgments** This work was funded by the Open Fund Project of the National Key Laboratory in University of Science and Technology Beijing of China (KF13-02) and the Natural Science Foundation of Hebei province (E2013209339).

**Open Access** This article is distributed under the terms of the Creative Commons Attribution 4.0 International License (<http://creativecommons.org/licenses/by/4.0/>), which permits unrestricted use, distribution, and reproduction in any medium, provided you give appropriate credit to the original author(s) and the source, provide a link to the Creative Commons license, and indicate if changes were made.

#### References

- Akiyama T (2000) In: K. Ishii, Advanced pulverized coal injection technology and blast furnace operation. Pergamon-Elsevier Science Ltd., Oxford, 169–173
- Assis PS, Vieira CB, Sobrinho PJN (2004) New developments for powder coal injection into the blast furnaces. *Process Metallurgy-Ironmak* 4:235–239
- Burton AW, Ong K, Rea T, Chan IY (2009) On the estimation of average crystallite size of zeolites from the Scherrer equation: a critical evaluation of its application to zeolites with one-dimensional pore systems. *Microporous Mesoporous Mater* 117(1–2):75–90
- Gong XZ, Guo ZC (2009) Effect of K<sub>2</sub>CO<sub>3</sub> and Fe<sub>2</sub>O<sub>3</sub> on combustion reactivity of pulverized coal by thermogravimetry analysis. *J Fuel Chem Technol* 37(1):42–47
- Gong XZ, Guo ZC, Wang Z (2009) Experimental study on mechanism of lowering ignition temperature of anthracite combustion catalyzed by Fe<sub>2</sub>O<sub>3</sub>. *CIESC J* 60(7):1707–1713
- He XJ, Zhang JL, Qi CL (2012) Kinetic analysis and effect of catalysts on combustion. *Iron Steel* 47(7):74–79
- Ichida M, Orimoto T, Tanaka T, Koizumi F (2000) Behavior of pulverized coal ash and physical property of dripping slag under high pulverized coal injection operation. *ISIJ Int* 17(2):325–332
- Indronil S, Muthukuma KM (2000) Blast furnace efficiency enhancer for pulverized coal injection. *Iron Steel Eng* 77(4):61–62
- Ishii K (2000) Advanced pulverized coal injection technology and blast furnace operation. Tokyo, Elsevier Science Ltd, p 73
- Liang ZG, He R, Chen Q, Xu XC, Sato J (2007) Fractal generation of char pores through random walk. *Combust Sci Tech* 179: 637–661
- Lu L (2001) Quantitative X-ray diffraction analysis and its application to various coals. *Carbon* 39:1821–1833

- Mathieson JG, Truelove JS, Rogers H (2005) Toward an understanding of coal combustion in blast furnace tuyere injection. *Fuel* 84(10):1229–1237
- Michael H (2002) Best effect of coke strength after reaction (CSR) on blast furnace performance. *Ironmaking Conference Proceedings*. Japan Tsukuba, 2–6
- Morimasa I, Tsuyoshi T, Fumio K (2001) Behavior of pulverized coal ash and physical property of dripping slag under high pulverized coal injection operation. *ISIJ Int* 41(6):325–332
- Shi L, Wang Y (2013) The promoting effect of La<sub>2</sub>O<sub>3</sub> on Ag/SiO<sub>2</sub> 3-catalyst for gas phase synthesis. *J Liaoning Normal Univ (Nat Sci Edition)* 36(4):512–515
- Takanohashi T, Terao Y, Iino M (1999) Irreversible structural changes in coals during heating. *Energy Fuels* 13:506–512
- Thoms PE, Phillip FB, Buchanan AC (1996) Does decarboxylation lead to cross-linking in low-rank coals. *Energy Fuels* 10(6):1257–1261
- Wang J, Shen MQ (2001) Modification effect of La<sub>2</sub>O<sub>3</sub> on Pd catalyst support. *J Tianjin Univ* 34(3):392–395